

Supporting Information

Surface hydrogen bonding can enhance the photocatalytic H₂ evolution efficiency

Xue Lu Wang,^[a,b] Wen Qi Fang,^[a,c] Hai Feng Wang,^[d] Haimin Zhang,^[b] Huijun Zhao,^[b] Yefeng Yao,^{*,[e]}
and Hua Gui Yang^{*,[a, b]}

Section S1: Crystal and chemical structures.

Samples	N [wt%]	C [wt%]	H [wt%]	Atom ratio (C/N)
g-C ₃ N ₄	58.46	33.88	2.09	0.676
CN-H1	56.75	32.53	2.33	0.673
CN-H2	55.55	32.20	2.30	0.676
CN-H3	57.55	32.62	2.05	0.672
CN-H4	48.20	28.26	2.45	0.684
CN-H5	33.99	21.39	2.54	0.734

Table S1. The results of elemental analysis for the pure g-C₃N₄ and CN-Hx.

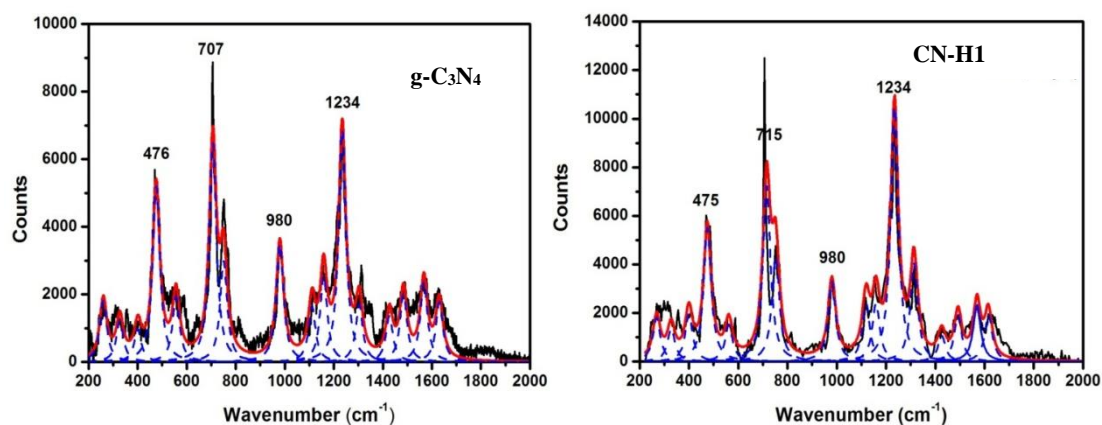


Figure S1. NIR Raman spectra (785 nm) of the pure g-C₃N₄ and CN-H1.

Analogous structure information was obtained in the NIR Raman spectrum (Fig. S1),^{R1} for example, two distinct peaks around 710 and 980 cm⁻¹, indicating the signals of s-triazine ring breathing modes.

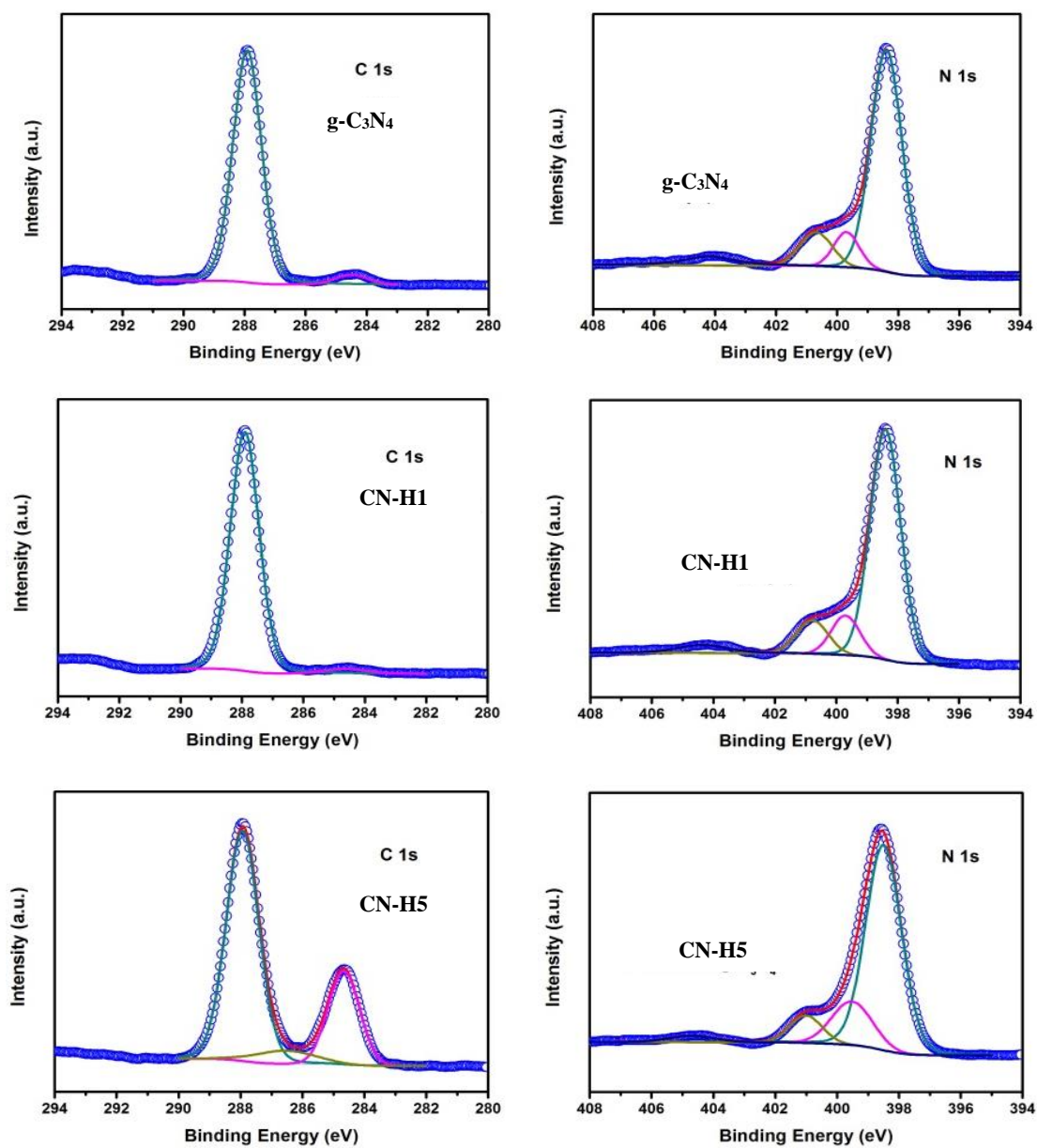


Figure S2. C 1s and N 1s XPS spectra of pure g-C₃N₄, CN-H1 and CN-H5.

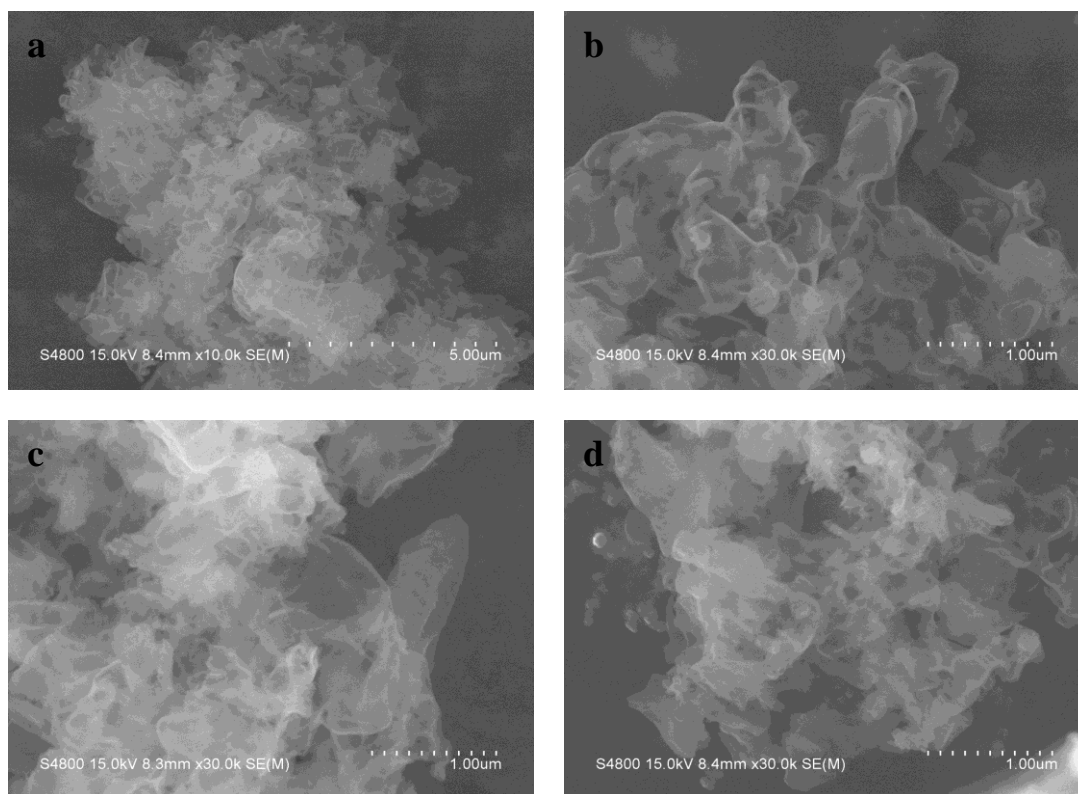


Figure S3. SEM images of (a, b) pure g-C₃N₄, (c) CN-H1 and (d) CN-H5.

Section S2: Solid-state NMR spectroscopy.

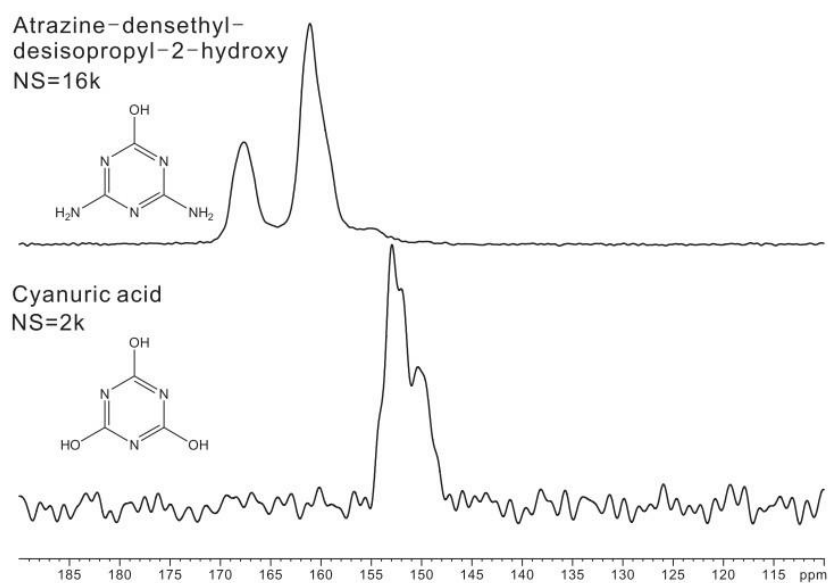
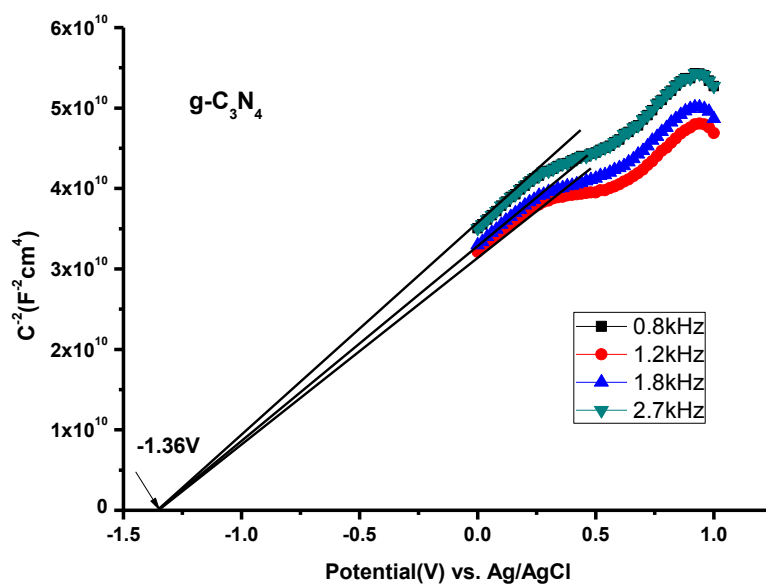


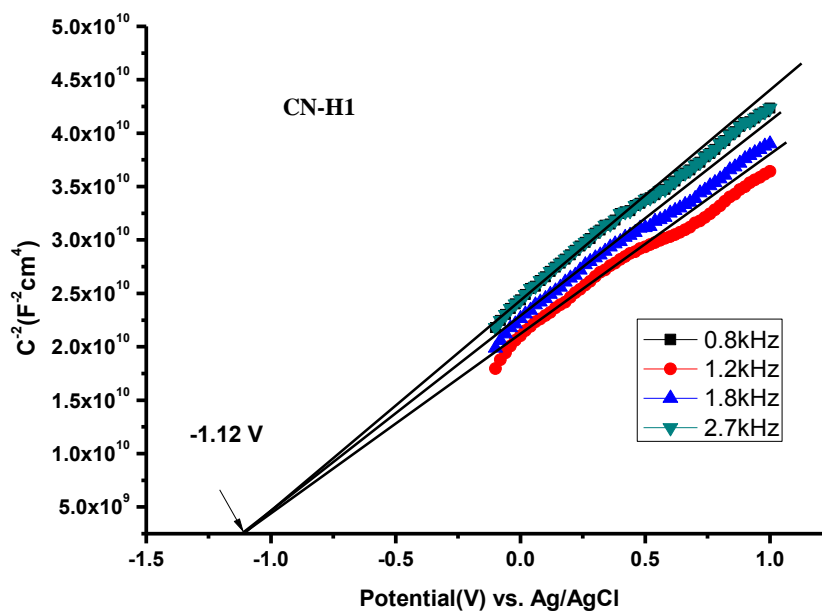
Figure S4. ^{13}C MAS solid-state NMR spectrum for Atrazine-densethyl-desisopropyl-2- hydroxy and cyanuric acid.

Section S3: Photocatalytic and optical absorption properties.

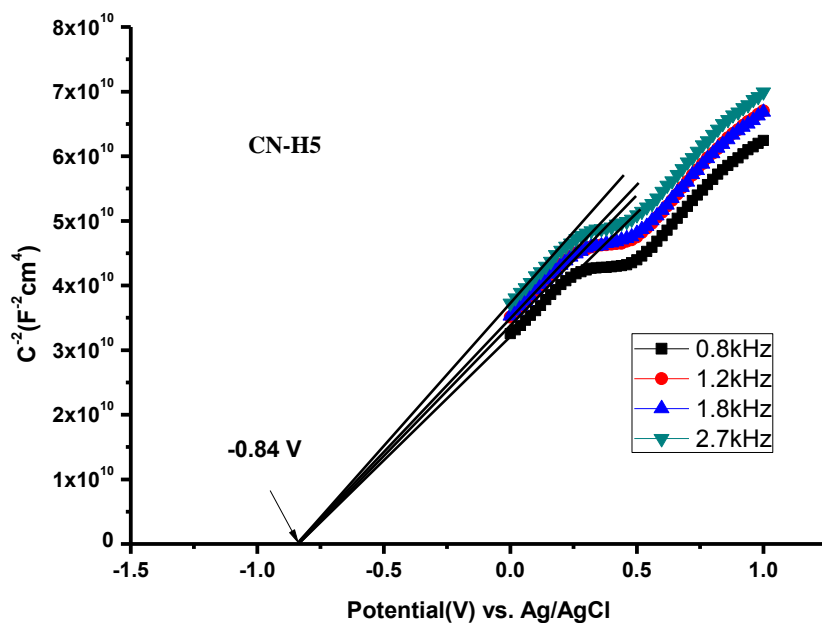
a



b



c



d

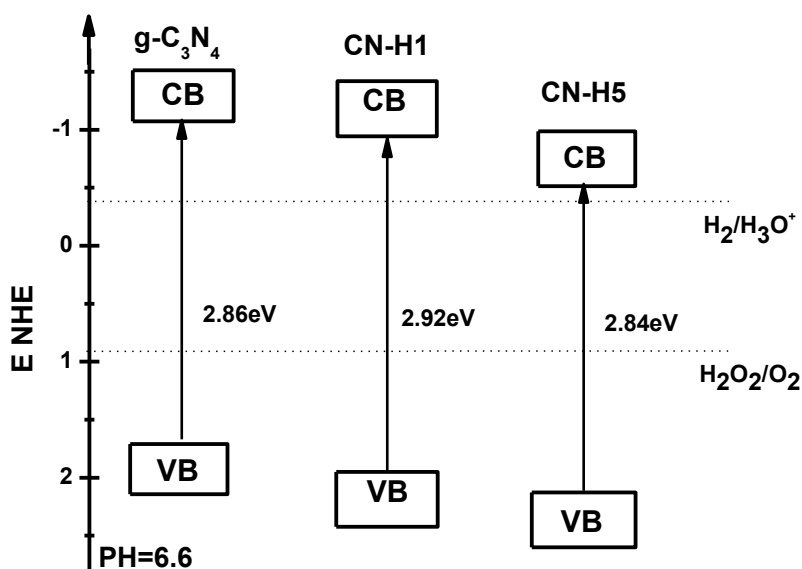


Figure S5. Electrochemical Mott-Schottky plots of (a) g-C₃N₄, (b) CN-H1 and (c) CN-H5 samples, and (d) Electronic band structure of g-C₃N₄, CN-H1 and CN-H5.

Positive slopes of Mott-Schottky plots (Fig. S6a, b, c) indicate the typical n-type characteristics for these organic semiconductors. The absolute energy scheme including conduction band (CB) and valence band (VB) positions were presented through combined the flatband position with the band gap energy

estimated from the UV-vis absorption spectrums (Fig. S6d). As observed from the UV-vis absorption spectra (Fig. S7), the CN-H1 shows a slightly blue shift of the intrinsic absorption edge in the nanosheets with respect to the g-C₃N₄.

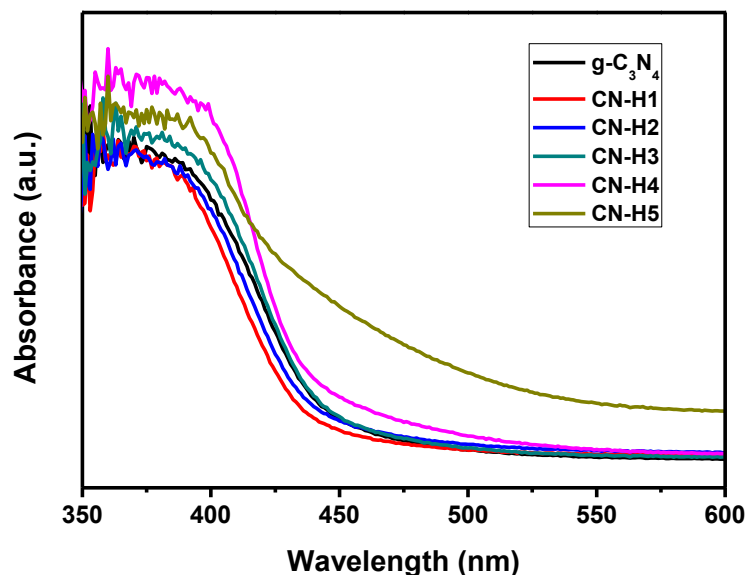


Figure S6. UV-visible absorption spectra of the g-C₃N₄ and CN-Hx samples.

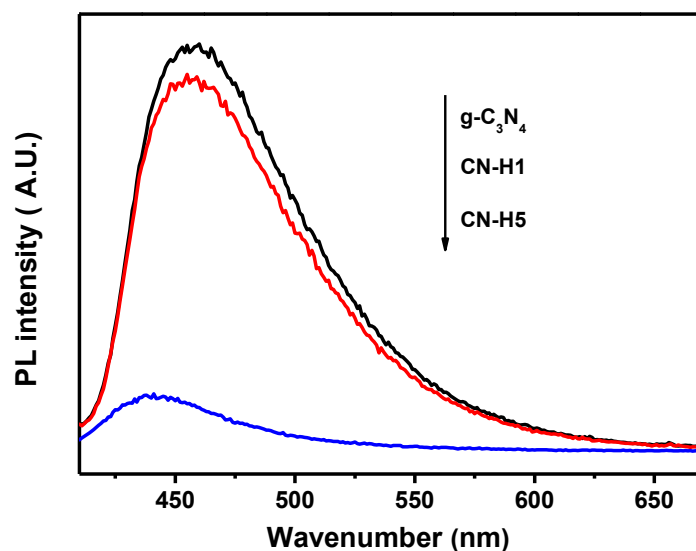


Figure S7. Room temperature PL spectra for pure g-C₃N₄, CN-H1 and CN-H5 ($\lambda_{\text{ex}} = 400$ nm)

To investigate if the Na⁺ in our CN-Hx catalyst has a promotional effect on the catalytic activity, we conducted another control experiment by replacing NaOH with KOH or NH₄OH. The photocatalytic

performances of the Na-free samples are comparable to that of CN-H1 (Fig. S9). Therefore, the Na⁺ can be unambiguously concluded that has no effect on the activity of g-C₃N₄.

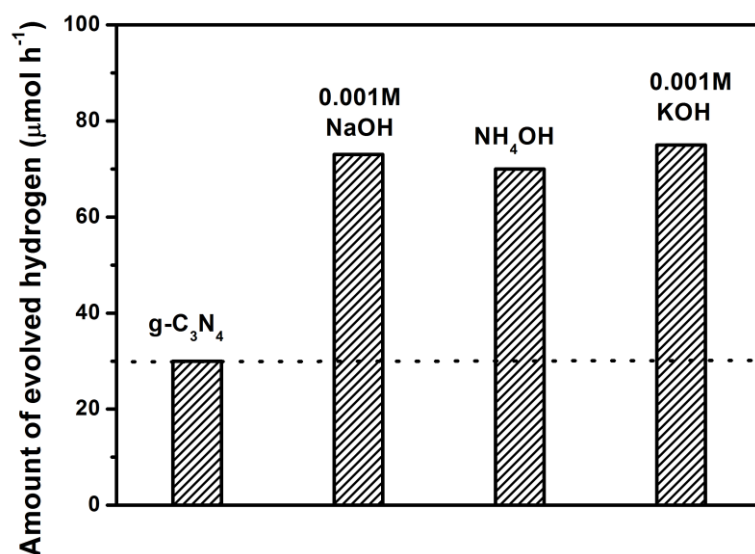


Figure S8. Photocatalytic activities of 30 mg pure g-C₃N₄, CN-H1, NH₄OH/g-C₃N₄, and 0.001M-KOH/g-C₃N₄ for hydrogen evolution under visible light irradiation ($\lambda > 420\text{nm}$).

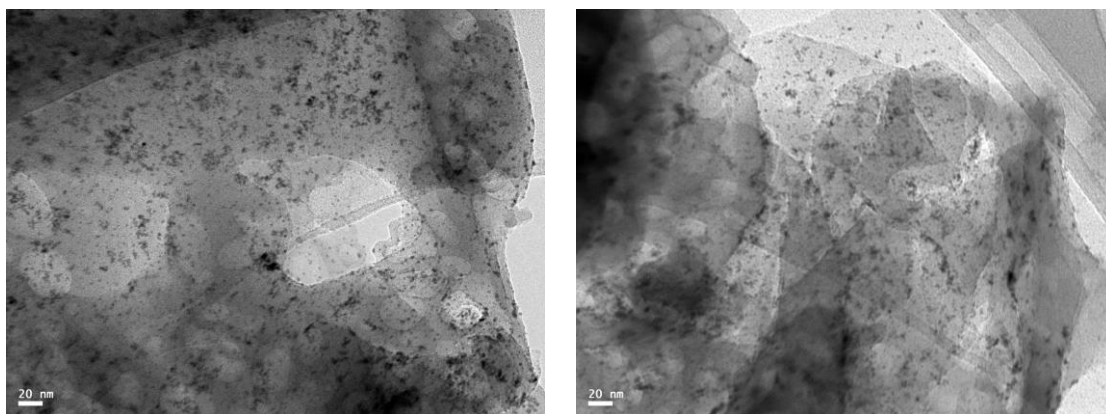


Figure S9. TEM images of A) pure g-C₃N₄/3 wt% Pt and B) CN-H1/3 wt% Pt samples.

Section S4: Density functional theory (DFT) calculations.

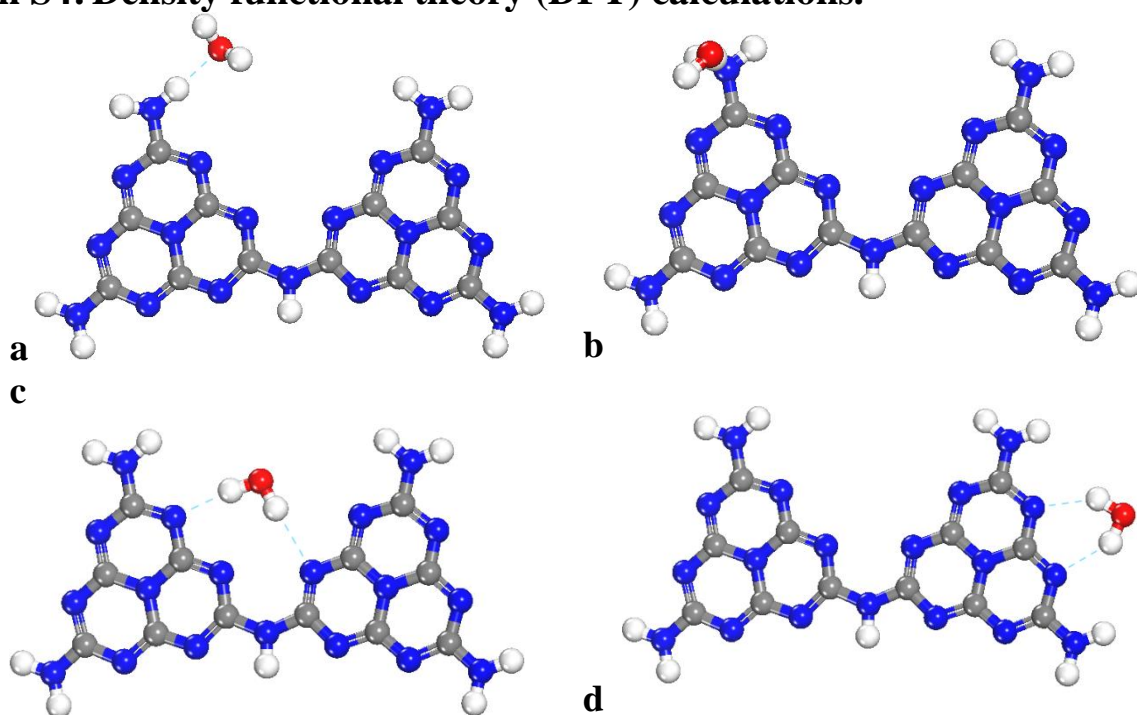


Figure S10. Optimized configurations of H₂O molecule interacting with the melem dimer by forming hydrogen bond at different positions.

With respect to the H₂O molecule, nearly all the possible configurations of H₂O interact with the melem dimer, one of the fragments constituting g-C₃N₄, were checked (see Fig. S10). It was found that H₂O can interact with the terminal -NH₂ group in melem structure to form two kinds of hydrogen bonds, i.e. either a HNH...OH₂ or H₂N...HOH hydrogen bond. The binding strength of both bonds is weak, while the former is a little stronger, giving a bond length for H...O bond ($d(\text{H}\cdots\text{O})$) of 1.95 Å. Further increasing the size of (H₂O)_n cluster to n=2 and 3, such a kind of interaction has no evident enhancement.

In addition, it is worth noting that H₂O molecule can interact with two C/N graphene ring of g-C₃N₄ by forming two hydrogen bonds at the skeleton edge-N atom (Fig. S10c, d), which is a little stronger than the HNH...OH₂ configure with one H bond at the end-NH₂ group. However, it is found that from DFT calculation that there exists an electrostatic repulsion between the N^{δ-} atom in the skeleton and OH⁻. Therefore, it can be speculated that a small number of OH⁻ would give little contribution in facilitating interaction with H₂O as such a kind of position in g-C₃N₄, while the presence of terminal -NH₂ or -NH at

the link site (not shown) can form hydrogen bond with O atom in H₂O or OH⁻ at different strength through their respective H atom, and thus the effect of hydrophilicity improvement induced by basicity treatment can be displayed. Further speaking, the hydrogen content of g-C₃N₄ should affect the basicity treatment efficiency.

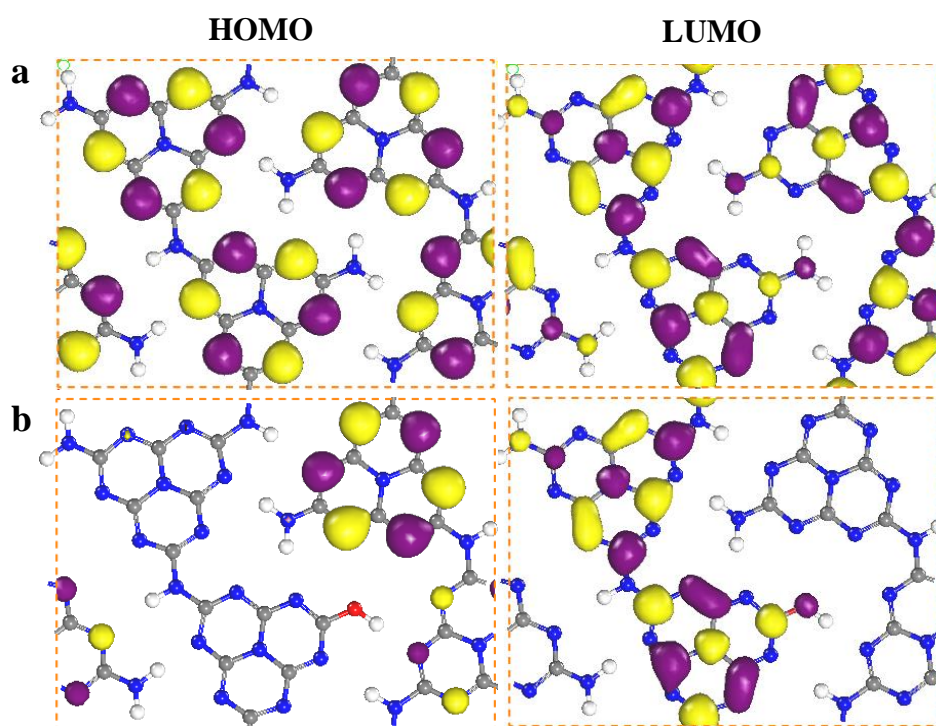


Figure S11. a) and b) represent the distribution of HOMO and LUMO orbital of pure polymeric melon and after substitution of end-NH₂ by OH⁻, respectively.

As shown in Fig. S11, polymeric melon consists of two one-dimensional hydrogen bonds between the H and N atoms. Similar with that of melon dimer, electronic structure calculations indicated that the wavefunction of the valence band of polymeric melon are derived from nitrogen p_z orbitals, and the conduction band consists predominantly of carbon p_z orbitals. Photoexcitation consequently leads to a spatial charge separation between the electron in the conduction band and the hole in the valence band. Introducing an OH in one chain of polymer melon by substituting an end-NH₂, the distribution of HOMO orbital would be reduced nearly at half, being localized at N atoms of the other chain, and the LUMO only distributed at the chain containing OH group, which may rationalize the decline of photocatalytic

activity of g-C₃N₄ after the concentrated NaOH treatment in term of the reduced active site number for photoexcitation and reaction.

References

R1 B. Yue, Q. Li, H. Iwa, T. Kako, J. Ye, *Sci. Technol. Adv. Mat.*, 2011, **12**, 034401.